Supporting Information

Koharudin et al. 10.1073/pnas.1002295107

SI Text

15d-PGJ2 Does Not Modify Every Cys Containing Protein. It has been assumed that any free protein thiol group may act as a nucleophile in the reaction with the electrophilic carbonyl moiety of the 15d-PGJ2 cyclopentenone ring. However, our results with the UCH-L1 Cys mutants contradict this notion. In order to probe this issue further, we selected two other completely unrelated proteins and subjected them to incubation with 15d-PGJ2, namely LKAMG (1), a designer lectin with a single, solvent exposed Cys and SERCA (Sarco(endo)plasmic reticulum Ca^{2+} ATPase) (2), containing six Cys residues with free thiol groups. No changes in the 2D ^{1}H-^{15}N HSQC spectra were observed after treatment with a twofold molar excess of 15d-PGJ2 (Fig. S7), indicating that no prostaglandin conjugation had occurred. LC-ESI-MS analysis confirmed that only unmodified, free protein was present.

The extensive aggregation of UCH-L1 upon conjugation with 15d-PGJ2 in vitro raises the question whether this event is physiologically relevant. Normal concentrations of prostaglandins in body fluids were found to be in pico- to nanomolar range (3), although it could well be that substantially increased levels of prostaglandins may be reached at the site of damage under pathological conditions, such as oxidative stress and inflammation (4). Although our NMR titration experiments were carried out at ~200 micromolar protein concentrations, unfolding is observed with substoichiometric amounts of 15d-PGJ2. Thus, the structure gets destroyed and aggregation occurs as soon as the protein is modified.

1. Koharudin LMI, Furey W, & Gronenborn AM (2009) A designed chimeric cyanovirin-N homolog lectin: Structure and molecular basis of sucrose binding. *Proteins* 77:904–915.
2. Olesen C, et al. (2007) The structural basis of calcium transport by the calcium pump. *Nature* 450:1036–1042.
3. Fukushima M (1990) Prostaglandin J2–anti-tumour and antiviral activities and the mechanisms involved. *Eicosanoids* 3:189–199.
4. Herschman HR, Reddy ST, & Xie W (1997) Function and regulation of prostaglandin synthase-2. *Adv Exp Med Biol* 407:61–66.

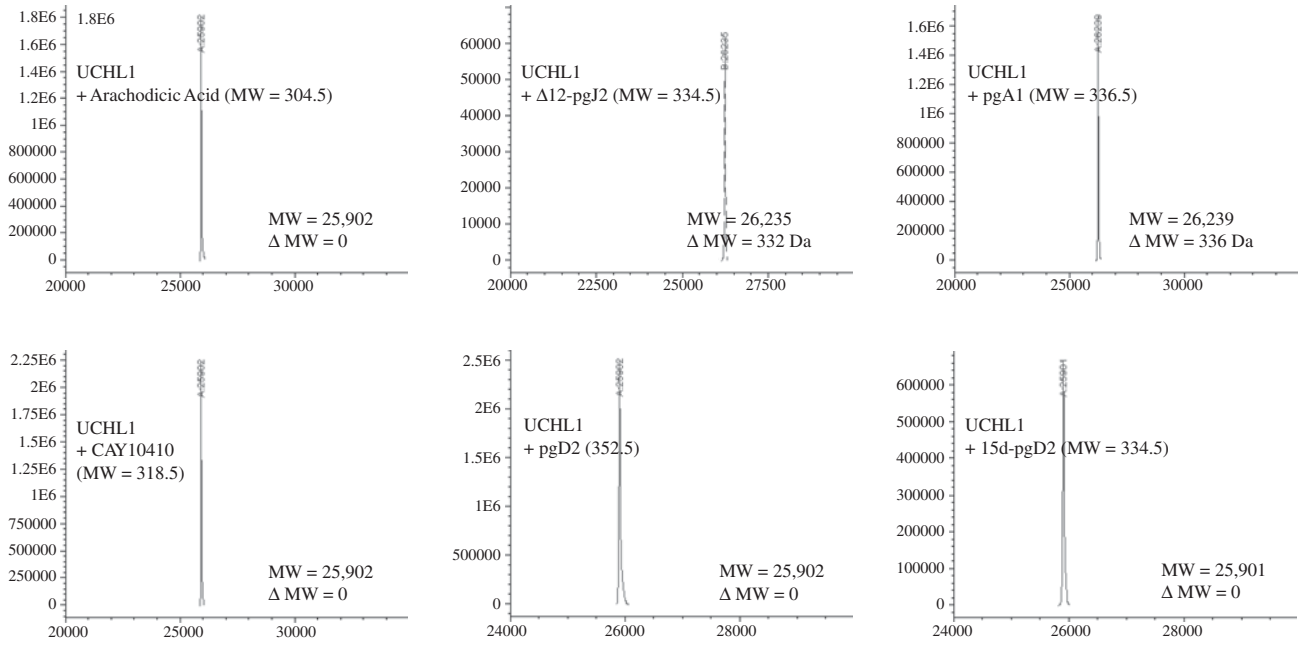

Fig. S1. ESI-MS analysis of UCH-L1 modification by arachidonic acid and various other prostaglandins. Species with a mass increase of 332 and 336 Da were only observed for Δ12-PGJ2 (334.5) and PGA1 (335.5), respectively, and no mass increase was observed for addition of arachidonic acid, CAY10410, PGD2, and 15d-PGD2, indicating that UCH-L1 is conjugated only by cyclopentenone prostaglandins of the A and J series.

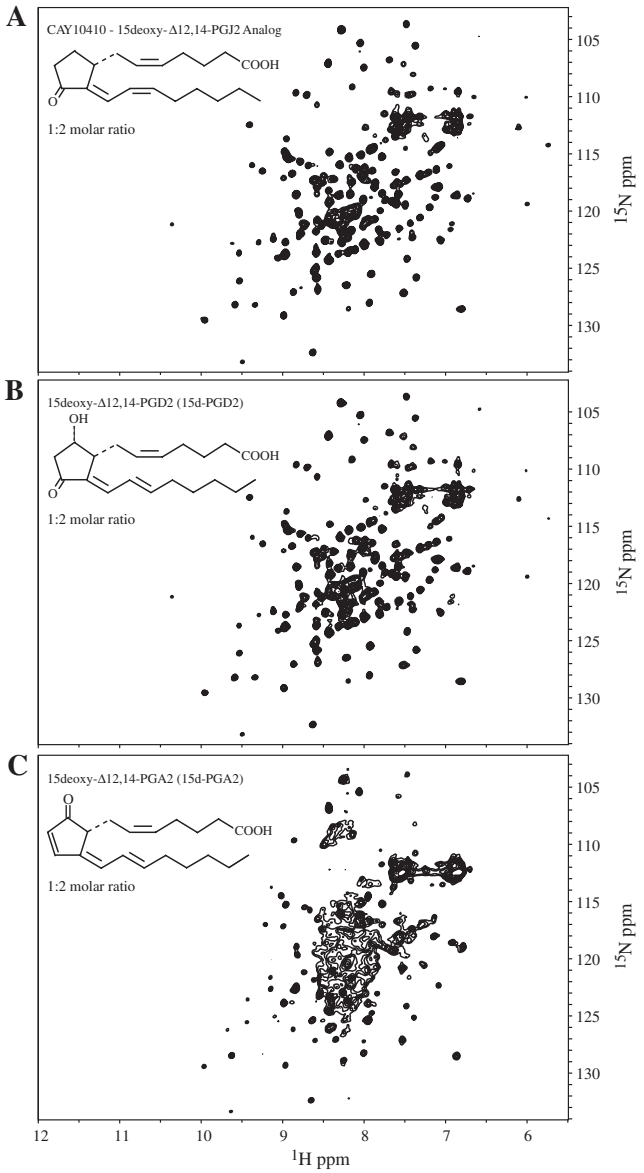

Fig. S2. NMR structural characterization of UCH-L1 aggregation upon conjugation with cyclopentenone prostaglandins. (*A*–*B*) 2D ^{1}H-^{15}N HSQC spectrum of UCH-L1 (0.2 mM protein, PBS buffer, pH 7.6, 298 K) exhibiting excellent chemical shift dispersion in the presence of twofold molar excess of CAY10410 (*A*) and 15d-PGD2 (*B*), indicating no conjugation of UCH-L1 to either of these molecules. (*C*) 2D ^{1}H-^{15}N HSQC spectra of UCH-L1 in the presence of twofold excess of 15d-PGA2, recorded under identical conditions as in *A* and *B*. Substantial resonance broadening is observed and the location of resonances in a narrow spectral region around 8–9 ppm (for ^{1}H) is indicative of unfolded/aggregated protein.

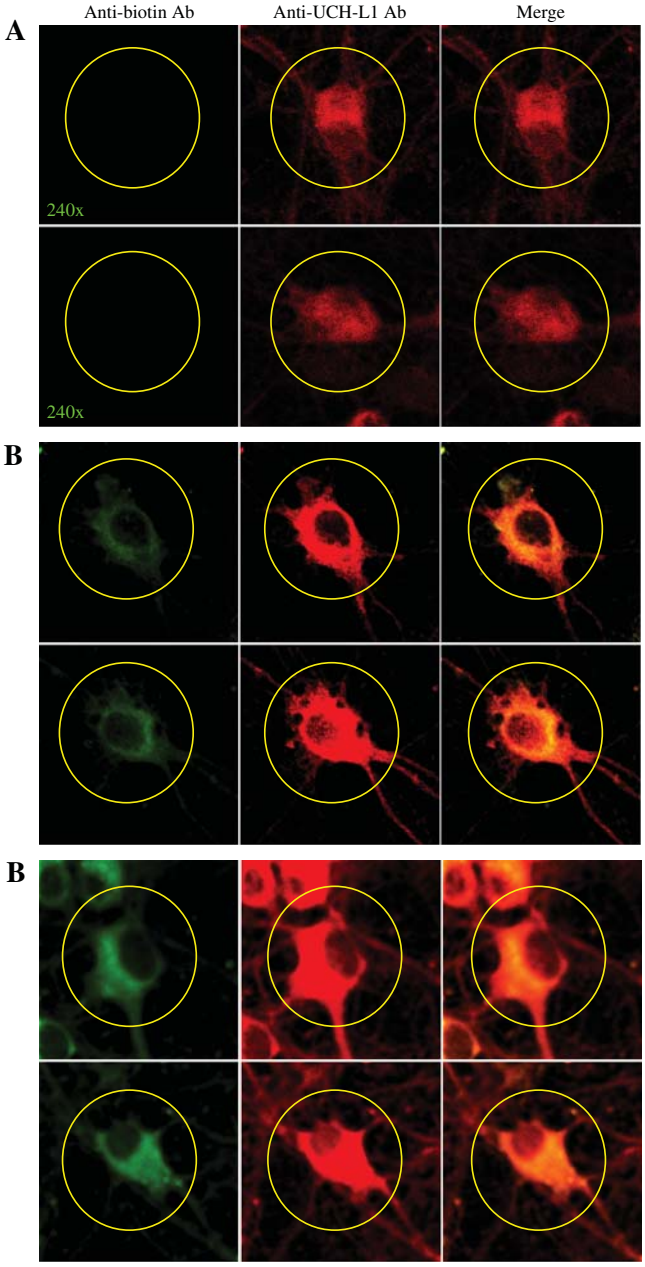

Fig. S3. In vivo aggregation of UCH-L1. Rat midbrain neuronal cells were treated with biotinylated-15d-PGJ2 and the distribution profile of UCH-L1 was examined. The presence of biotinylated-15d-PGJ2 and endogenous UCH-L1 in rat midbrain neuronal cells was detected using antibiotin (left) and anti-UCH-L1 (middle) antibodies and colocalization is illustrated at right. (*A*–*C*) UCH-L1 distribution profiles in the absence (*A*) and after treatment with 12 μM of 15d-PGJ2 for 12 h (*B*) and 24 h (*C*), respectively. The images were obtained at 240x magnification.

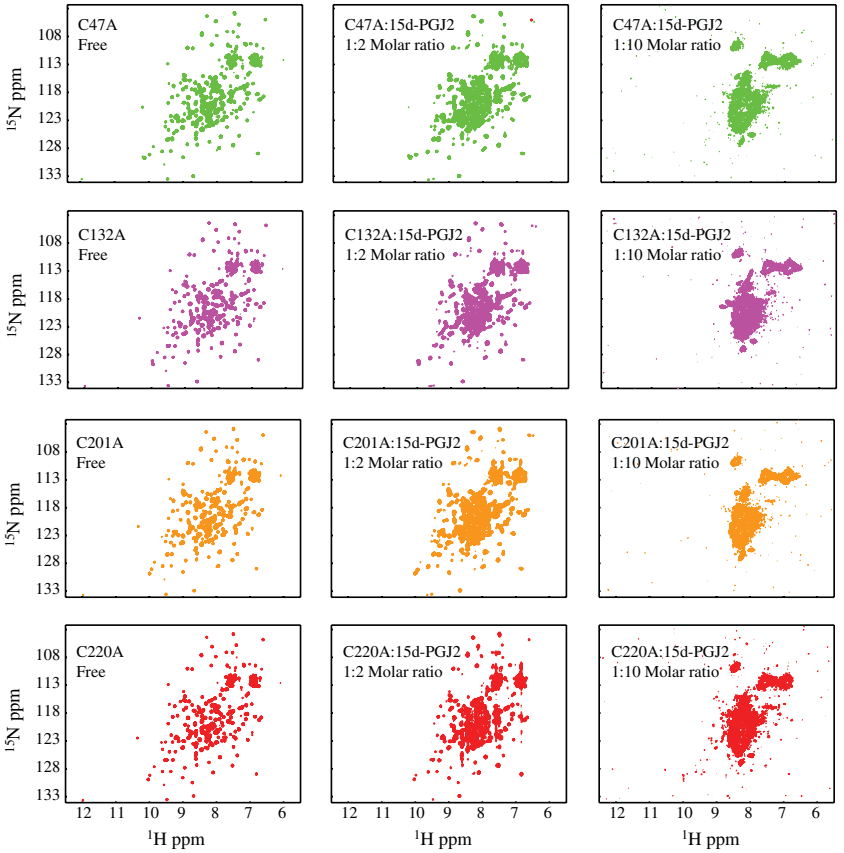

Fig. S4. Aggregation of UCH-L1 C → A mutants. The ^{1}H-^{15}N 2D HSQC spectra for four other C → A UCH-L1 mutants were recorded at 0.2 mM protein concentration in the absence (left column) and in the presence of twofold (middle column) and 10-fold (right column) molar excess of 15d-PGJ2 in 1x PBS buffer (pH 7.6) at 298 K; C47A (*Green*), C132A (*Magenta*), C201A (*Orange*), and C220A (*Red*). Aggregation is observed for all these mutants.

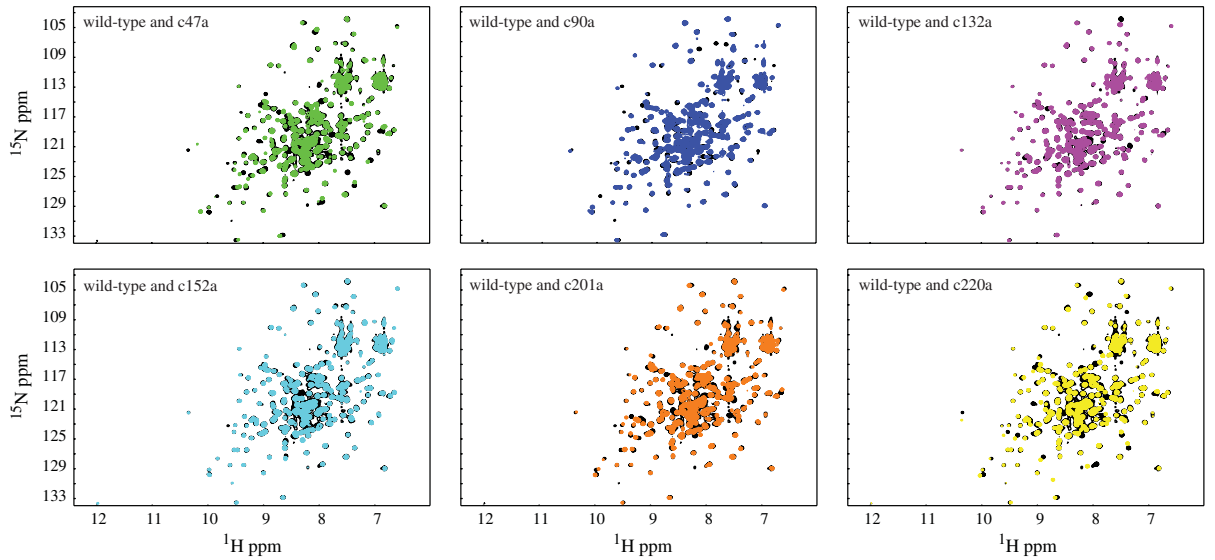

Fig. S5. Superposition of the ^{1}H-^{15}N 2D HSQC spectra of wild-type UCH-L1 and individual C → A mutants. The structures of the mutants are not affected significantly compared to wild-type protein as indicated by well-resolved amide resonances. Only very small shifts were observed for residues surrounding each mutation site. Spectra for wild-type protein and C47A, C90A, C132A, C152A, C201A, and C220A mutants are shown in black, green, blue, magenta, cyan, orange, and yellow, respectively. All spectra were recorded at 0.2 mM protein concentration in 1x PBS buffer (pH 7.6) at 298 K.

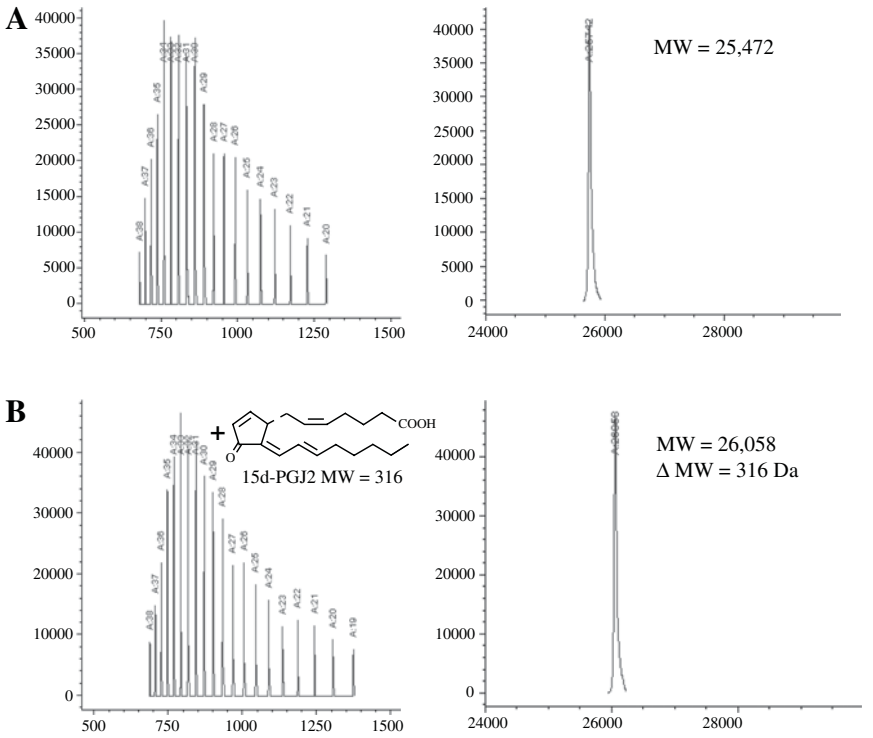

Fig. S6. ESI-MS analysis of the reaction between the UCH-L1 $A_{47}A_{90}A_{132}C_{152}A_{201}A_{220}$ mutant and 15d-PGJ2. Species with masses of 25,472 Da and 26,058 Da are observed for free (expected mass 25,473 Da) (*A*) and for 15d-PGJ2-conjugated (expected mass 26,058 Da) (*B*) mutant protein, respectively, confirming that the thiol group of C152 serves as the sole nucleophile in UCH-L1 for 15d-PGJ2 conjugation.

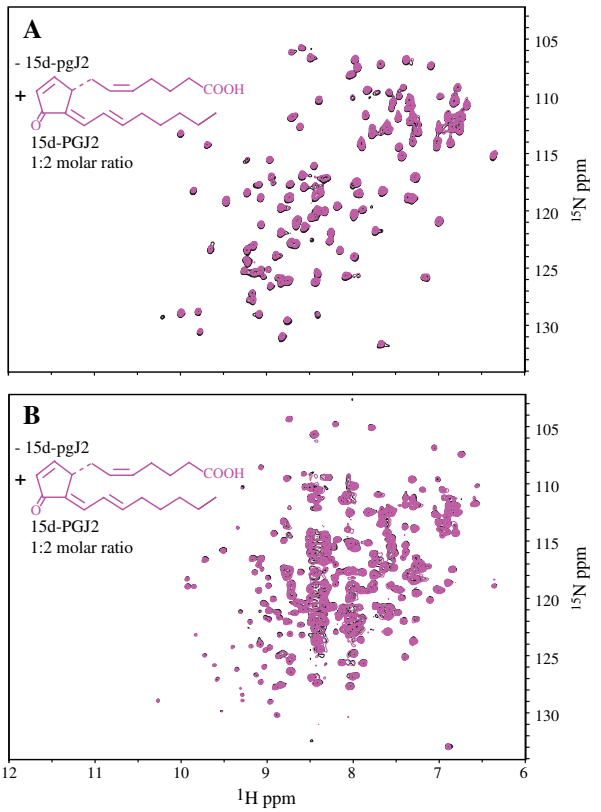

Fig. S7. NMR analysis of 15d-PGJ2 treatment of LKAMG and SERCA. No significant chemical shift changes were observed in the ^{1}H-^{15}N 2D HSQC spectra of LKAMG (*A*) and SERCA (*B*) in the absence (*Black*) and presence of twofold molar excess of 15d-PGJ2 (*Magenta*). All spectra were recorded in PBS buffer (pH 7.6) at 298 K.

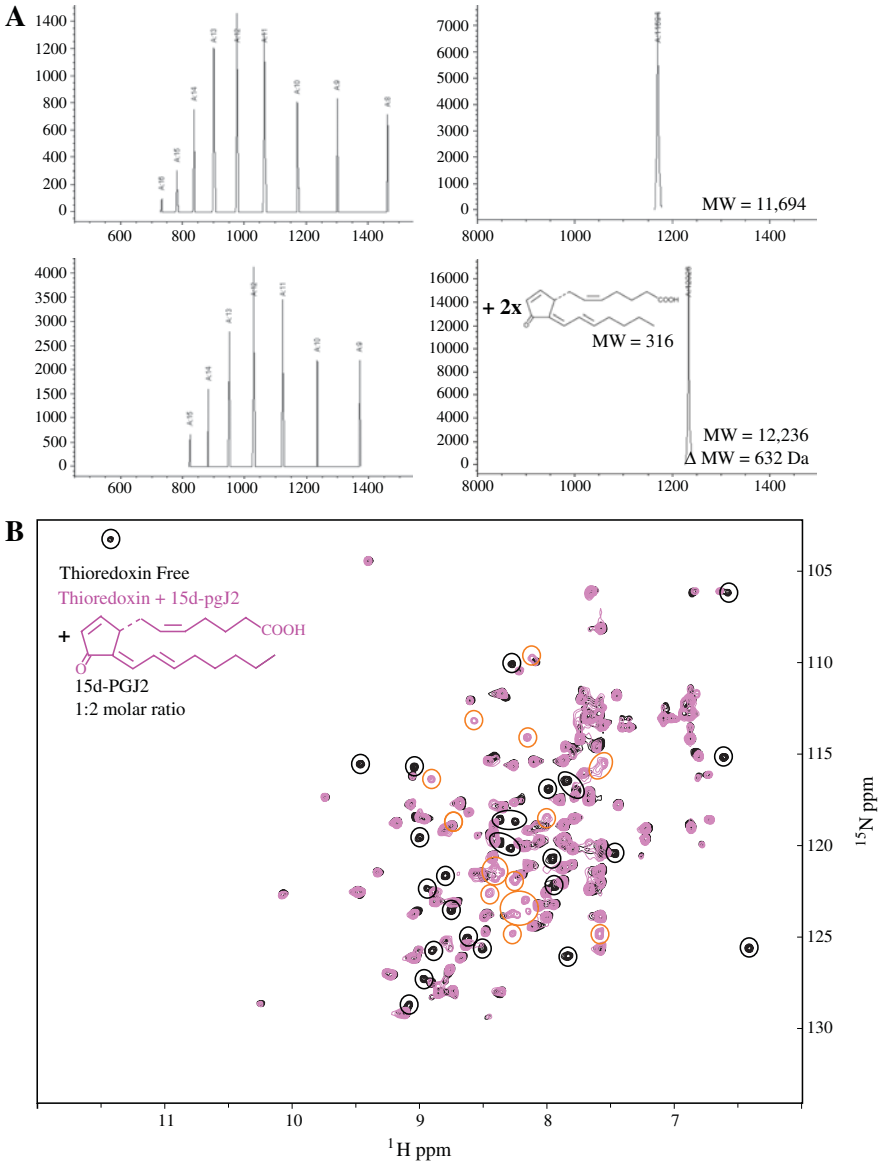

Fig. S8. ESI-MS and NMR analysis of thioredoxin modification by 15d-PGJ2. (*A*) ESI analysis of thioredoxin after treatment with 15d-PGJ2 indicates that two molecules of 15d-PGJ2 are conjugated per molecule of thioredoxin, evidenced by a mass increase of 632 Da. (*B*) Superposition of the ^{1}H-^{15}N 2D HSQC spectra of free (*Black*) and 15d-PGJ2 modified thioredoxin (*Magenta*). The observed chemical shift changes indicate a conformational change but not unfolding/aggregation of thioredoxin.

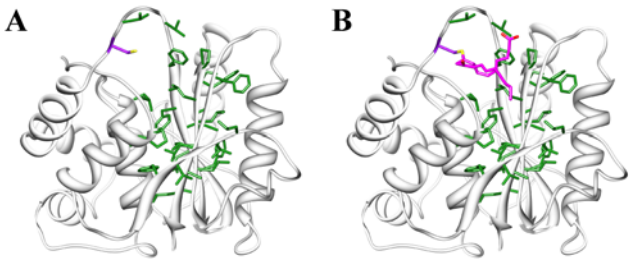

Fig. S9. Structure of UCH-L1 highlighting hydrophobic residues at the UCH-L1 domain interface around C152. (*A*) A large number of hydrophobic amino acids (colored in *Green*) are present surrounding the C152 residue, contributing to the hydrophobic core at the interface between the two lobes of UCH-L1. (*B*) Location of the acyl chains of 15d-PGJ2 when attached to C152.